As originally published in the International Conference on Soldering and Reliability Preedings.

BOARD LEVEL RELIABILITY EVALUATION OF LOW SILVER (AG) CONTENT LEAD-FREE SOLDER JOINTS AT LOW STRAIN RATES

Vikram Srinivas, Nicholas Williard, Preeti Chauhan and Michael Osterman
Center for Advanced Life Cycle Engineering, Department of Mechanical Engineering
University of Maryland
College Park, MD, USA

ABSTRACT

To improve the durability of lead free solder joints under high strain rates, such as drop and shock loading, some area array manufacturers have converted to low silver (Ag) content tin silver copper (SAC) solder spheres instead of the commonly accepted SAC305 solder. While the lower silver content SAC solder joints may address high strain rate shock loads, the durability of these joints under low strain rates has to be taken into consideration. The objective of this study is to assess the reliability under loading conditions with strain rates several orders of magnitude below that observed in drop testing. To this end, thermo-mechanical loading induced by temperature cycling (-55°C to 125°C) and mechanical loading induced by cyclic board level mechanical torsion were considered. Test vehicles were assembled using SAC305 solder paste with eight peripheral ball grid array packages (BGA) per printed wiring board with SAC105, SAC125Ni and SAC305 solder spheres. Four test specimens per type were assembled. Two of test specimens of each solder combination were then subjected to temperature cycling, while the remaining two were subjected to mechanical torsion. In-situ electrical resistance monitoring was performed on the low electrical resistance paths formed by the individual packages and the printed wiring board. Statistical analysis was conducted on cycles to failure data collected from the defined tests. A drop in fatigue durability with decrease in silver content in the solder spheres was observed for both thermo-mechanical and mechanical loading.

Keywords: Lead-free electronics, Rework process, BGA, Mechanical Bend test, Weibull analysis

INTRODUCTION

Restriction of Hazardous Substances (RoHS) legislation passed by the European Union triggered a dramatic change in the electronics industry with the most notable being the removal of lead from board and part surface finishes as well as the introduction of large scale production of lead-free soldered electronic assemblies. Literature discusses this shift to lead-free electronics considering the technical and legislative issues related to lead-free electronics [1].

Prior to the RoHS legislation, eutectic SnPb was the solder of choice for most applications. With the advent of RoHS, the tin-silver-copper (SAC) alloy has been the focus of research for replacing tin-lead solder. Early studies focused on 95.5% tin 4% silver 0.5% copper (SAC405) or some similar composition. Later studies focused on 96.5% tin 3% silver 0.5% copper (SAC305). With the conversion imminent, SAC305 appeared to be the preferred lead-free solder [1]. However, mechanical fragility of SAC305 solder joints under drop/shock conditions has resulted in an examination of lower silver content SAC solders [2]. While the reduction in silver appears to improve solder joint reliability under drop/shock, it increased the creep strain under temperature cycling which is expect to reduce solder joint reliability under conditions of low-strain rate and extended dwells [3].

Literature documents improved interconnection durability of assemblies using reduced-Ag content SAC solder alloys under high strain rate. Results include tests based on drop tests [4-6], high speed bend tests [7], high-speed ball shear [8] and high-speed ball pull [9]. Performance of reduced-Ag SAC solder at high strain rates has been discussed by D. Suh et al [10] and M. Reid [11]. The strain rate commonly observed under these tests at solder level has been described to be in the order of $10^{-2}-10^{-1}\mu\varepsilon/s$ [12]. Under high-strain rate mechanical shear loading at board level reduced-Ag SAC has been shown to perform better than SAC305 [13]. While the focus of reduced-Ag SAC solders has been to solve the drop/shock fragility issue, the ability of these new solders to handle low strain rate repetitive cycling has received less attention.

Though reduced-Ag SAC alloys show promise in improving drop/shock fragility, they have a detrimental effect in low strain rate cyclic loading. Available literature on durability of reduced-Ag SAC alloys under low strain rate cyclic loading has been primarily based on thermal cycling tests [14, 15]. The impact of ramp rate (strain rate) in thermal cycling has been discussed by Fan et al [16]. The strain rate under thermal cycling tests at solder level has been estimated to be in the order of $10^{-6}-10^{-5}\mu\varepsilon/s$ [17]. As discussed, high strain rate performance of low silver SAC solder joints has been documented [2- 12] but the low strain rate performance needs further study. Therefore, there is a need to understand board level reliability of reduced-Ag solder joints at low strain rates, especially under mechanical loading.

In this paper, the reliability of ball grid array (BGA) solder joints with reduced-Ag SAC solders under low strain rates using both, temperature cycling and cyclic mechanical torsion is examined. IPC provides outlines for temperature cycling tests for electronic packages in its standard [18, 26]. Solder joints under temperature cycling experience cyclic loading due to differences in coefficient of thermal expansion between materials involved in the assembly. Mechanical torsion has also been used to examine the durability of solder interconnects [19-21]. The strain rate in solder interconnects under mechanical torsion is estimated to be higher than thermal cycling and lower than drop test for chosen loading conditions. In the remainder of this paper, the test vehicles and test methods are presented. The results from data analysis of these tests will be discussed. Finally, the conclusions of the study are presented.

TEST VEHICLE

The test vehicle used in this study consists of an 8″ × 4.5″ × 0.062 inch printed wiring board (PWB) with eight defined package positions. Each PWB was constructed with Isola 370HR board laminate with package attach land patterns coated with organic solderability preservative (OSP) board finish. A test vehicle is shown in Figure 1.

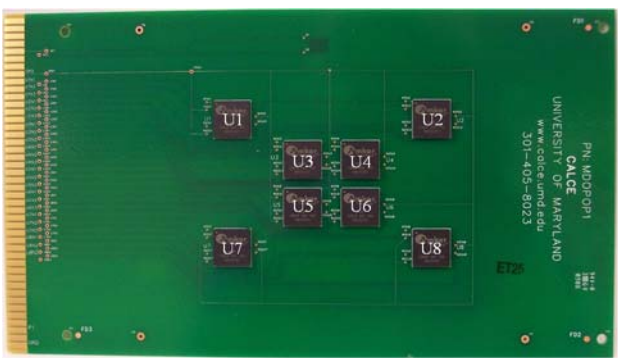

Figure 1: Test vehicle

For these imposed tests, two different 12x12 mm packages were used. The first package, Type A, was a 0.65 mm pitch peripheral BGA package with 128 solder spheres (18×18 matrix) and a stand-off height of 0.3 mm. The type A packages contained two dies stacked to represent conventional memory applications. The bottom die in this configuration had a side of 5.9 mm and thickness of 0.07mm while the stacked die had a side of 4.7 mm and thickness of 0.07 mm. The type B package was a 0.5 mm pitch peripheral BGA package with 305 solder spheres (23×23 matrix) and a stand-off height of 0.2 mm. These packages contained a single die to represent conventional processor applications with a side of 6.3 mm and thickness of 0.1 mm.

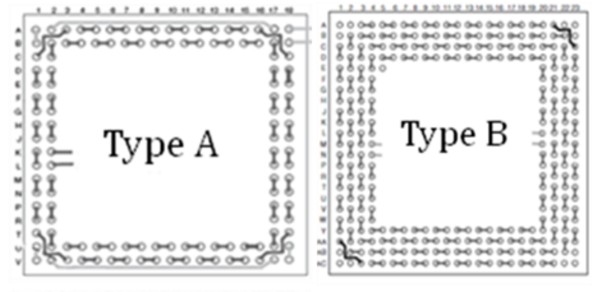

Figure 2: Schematic of package types A and B

As assembled type A packages had two daisy chained nets that allow continuous low electrical resistance monitoring during test. The corner 12 solder balls of the type A package formed the first daisy chain, while the remaining solder balls in the type A package formed the second daisy chain. The type B package's solder interconnects were routed to form a single daisy chain. During the cyclic loading tests, the nets were monitored independently to allow identification of the first daisy chained net to experience failure in the package. The schematic of the package with the daisy-chain net layout is depicted in Figure 2.

Type A BGA packages were procured with either SAC105 (98.5%Sn + 1.0%Ag + 0.5Cu) or SAC305 (96.5%Sn + 3.0%Ag + 0.5%Cu) solder spheres. Type B BGA packages were procured with either solder spheres of SAC125Ni (98.25%Sn + 1.2%Ag + 0.5%Cu+0.05%Ni) or SAC305. SAC305 solder paste was used for all assemblies. Hence the final composition for the reduced-Ag solder joints would include a higher Ag content than solder sphere composition. The reflow profile for the SAC305 solder has been shown in Figure 3 with thermocouples (T1, T2 and T3) at locations U2, U4 and U7 as referenced in Figure 1.

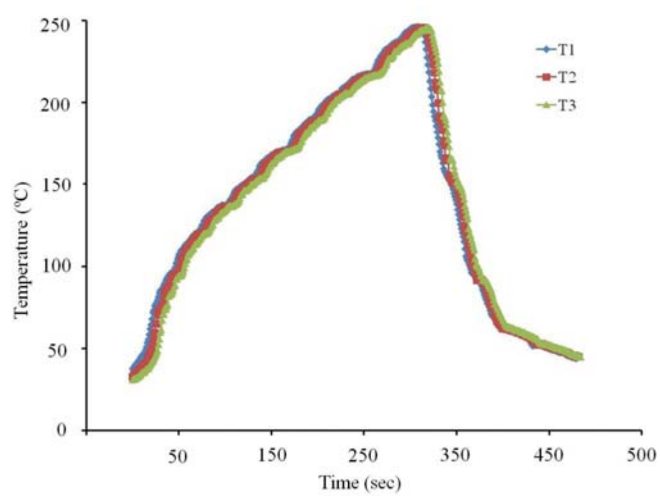

Figure 3: Reflow profile for SAC305 solder paste

The breakdown on test assemblies for the study is shown in Table 1. Four test specimens were assembled for each type to allow two test specimens each for thermal cycling (TC) and mechanical torsion test (TT).

Table 1: Test Assemblies

Board Type	Solder Alloy	Stand-off height (mm)	Parts tested	
			TC	TT
Type A	SAC305	0.3	16	16
Type A	SAC105	0.3	16	16
Type B	SAC305	0.2	16	16
Type B	SAC125Ni	0.2	16	16

THERMAL CYCLING TEST

All specimens were preconditioned at 100°C for 24 hours prior to test. Thermal characterization of the chamber using themo-couples was performed before testing to assure programmed temperature profile match the desired test profile. The test samples were placed on racks Figure 4 to provide air flow around each specimen. High temperature insulated wiring was used to connect test boards to an Agilent 34980A multifunction switch/ measure unit for in-situ resistance monitoring. Individual electrical resistance nets for the packages under test were monitored with a sampling rate of two minutes.

Figure 4: Thermal chamber

All components were cycled from -55 to 125°C with a ramp rate of 10°C/min and a max and min dwell of 15 minutes as per IPC-SMT-785 [18]. Multiple thermocouples were placed strategically in the board racks to monitor chamber temperature during the test. Thermo-couple data from the chamber are presented in Figure 5.

Resistance data was collected and processed in order to record the time to failure for each component. A resistance net was considered to failure at the first interruption of electrical resistance above 25 ohms from the base resistance confirmed by 9 additional interruptions within an additional 10% of cyclic life. The test was stopped after resistance nets for all packages had recorded failures.

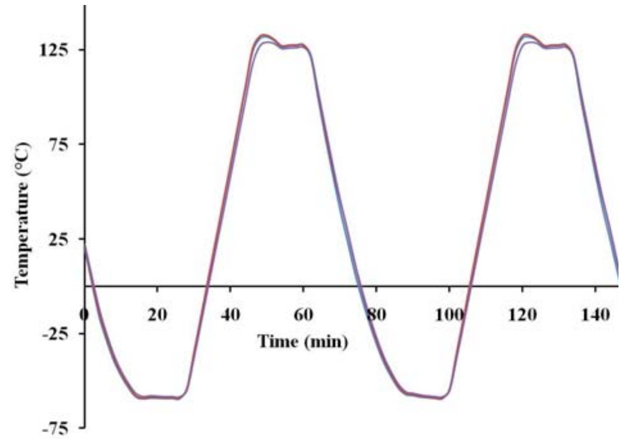

Figure 5: Temperature load profile

TORSION TEST

Torsion load on the PWB is applied using a custom test system that provided a static platform and controlled rotary platform. The rotary platform is controlled using a servo motor and angular displacement, angular velocity and angular acceleration with feedback. This test system allows control of peak-to-peak board strain and average strain rate. This technique has been described with strain analysis in previous publications [22, 23]. The strain across the solder joint can be estimated as described in literature [24, 25]. A picture of the test setup is shown in Figure 6.

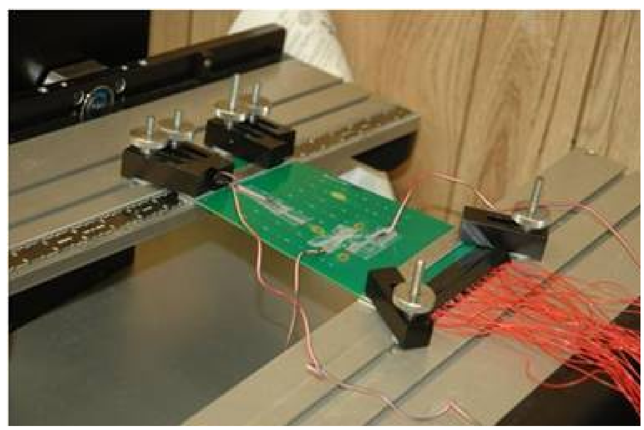

Figure 6: Torsion test setup

For this study, an angular deflection of 4.5° full cyclic load was selected at angular velocity of 1°/s and angular acceleration of $1°/s^2$. This setting approximately translates into board shear strain of 1000 µstrain units at an average strain rate of 50 µstrain units/sec. Based on finite element analysis results from previous studies the area array packages are categorized into two different stress levels labeled as stress level I and stress level II and identified in Figure 7. This is due to the difference in distance from axis of rotation of the test specimen.

The failure criteria used for the torsion tests is based on IPC-9701 [26]. A 20% increase in nominal resistance for 5 successive cycles was defined as failure. All test specimens were cycled to 100% failure. Two strain gages were affixed to the unpopulated side of each specimen adjacent to one BGA package at stress level I and II.

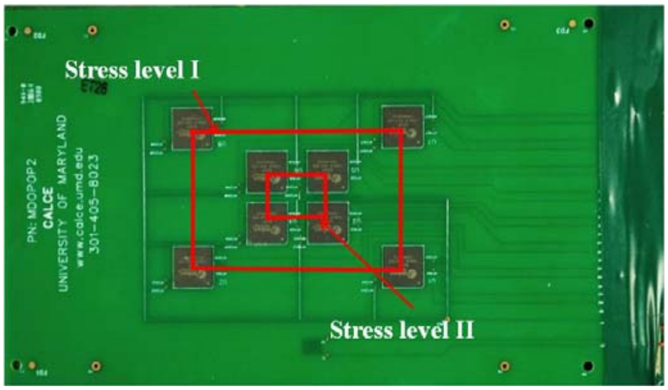

Figure 7: Stress levels under torsion on PWA

RESULTS

Using the defined failure criteria and the monitored resistance data, the cycles to failure were established for each net of the tested assemblies. The failure data was then plotted with a Weibull 2-parameter distribution.

Probability of failure plots with the temperature cycle test data are shown in Figure 8. For type B packages, characteristic life (cycles to 63% failure) of SAC305 solder joints is observed to be 26% higher than the same metric for the SAC125Ni solder joints. For type A packages, the characteristic life (cycles to 63% failure) for the SAC305 solder joints is observed to be 54% higher than the same metric for the SAC105 solder joints. We can conclude that temperature cycling fatigue durability follows the order of SAC305, SAC125Ni followed by SAC105. Also of interest is that the durability of type A BGAs has higher durability than type B for the same solder sphere of SAC305 by 60%. The reason for this is the higher stand-off height of type A (0.3 mm) compared to type B (0.2 mm) leads to drop in shear strain across the solder ball stand-off height.

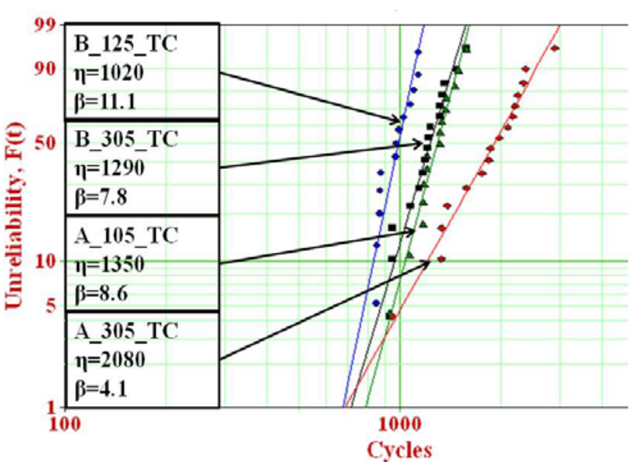

Figure 8: Durability under thermal cycling for test matrix

Figure 9 shows the probability of failure plot for the torsion test results with components placed at stress level I. Similar to the temperature cycling results, the SAC305 type B packages are found to have a higher fatigue life compared to the SAC125Ni type B packages. In this case the characteristic life (cycles to 63% failure) for the SAC305 type B packages is 29% higher than the same metric for the SAC125Ni type B packages. For type A packages, the characteristic life (cycles to 63% failure) for the SAC305 solder is observed to be 170% higher than the same metric for the SAC105 packages under mechanical torsion. The trend for mechanical torsion fatigue durability is consistent with thermal fatigue durability. However, the type B BGAs exhibit higher durability than type A for the same solder sphere of SAC305 by 180%. The increased mechanical torsion durability of the type B package despite the higher standoff is likely due to the reduced package thickness, higher IO count and the absence of the overmold at the perimeter of the package.

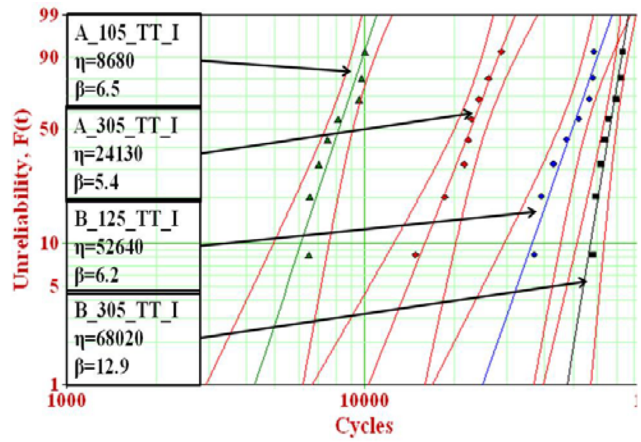

Figure 9: Durability under torsion testing for test matrix at stress level I

Type B packages failure data from thermal cycling test and torsion testing are plotted in Figure 10. This plot allows us to compare SAC305 and SAC125Ni under thermal cycling and mechanical torsion cycling. It is observed that SAC305 outperforms SAC125Ni in both these loading conditions. When failure data from thermal cycling test and torsion testing for type A packages are plotted, SAC305 is observed to outperform SAC105 solder.

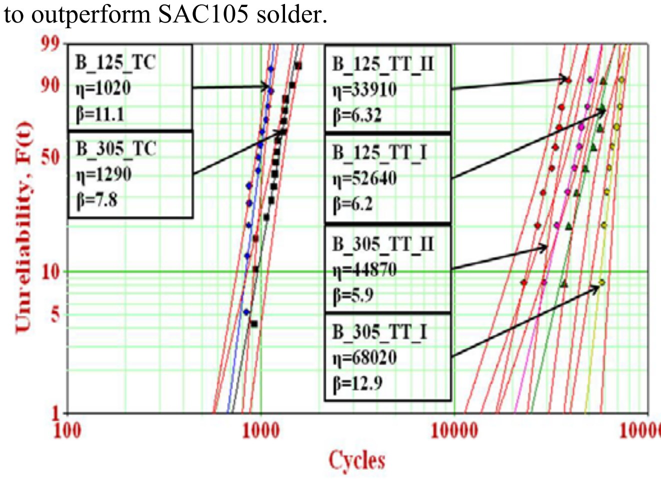

Figure 10: Durability under torsion testing and thermal cycling for type B packages

Figure 11 plots the failure data for all SAC305 solder under different packages and loading conditions. While type A outperforms type B packages under temperature cycling, a reversal in trend is observed in mechanical torsion cycling results. For the temperature cycling test, the higher standoff height provides the likely explanation for the longer life when comparing type A with type B BGA packages under test. For the mechanical torsion, the thicker package likely overcomes the advantage of standoff height resulting in type B BGA packages outlasting type A BGA packages. For mechanical torsion, the BGA position on the test board also influences interconnect durability. Here, the packages near the center of the board experience lower interconnect durability likely due to a higher imposed cyclic strain. A more detailed description of torsion tests results can be found was provided in an earlier publication [23].

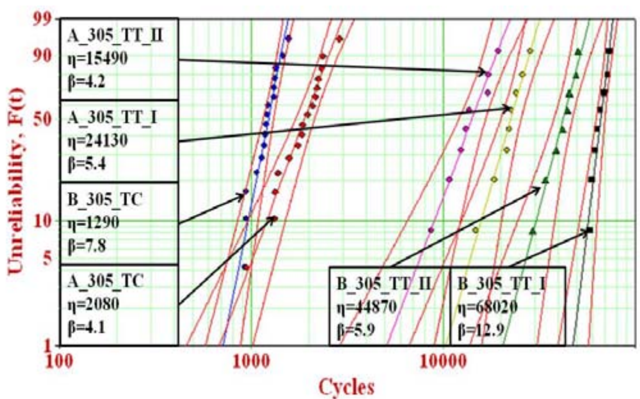

Figure 11: Durability under torsion testing and thermal cycling for SAC305 packages

SUMMARY AND CONCLUSIONS

Under temperature cycle test, durability was observed to drop with a reduction in silver (Ag) content i.e. SAC305 (96.5%Sn + 3.0%Ag + 0.5%Cu)> SAC125Ni (98.25%Sn + 1.2%Ag + 0.5%Cu+0.05%Ni) > SAC105 (98.5%Sn + 1.0%Ag + 0.5Cu Under mechanical torsion cycling, durability of tested solders was observed to follow the same trend. SAC305 solder joints exhibits higher characteristic life in both type A and B configurations compared to mixed reduced-Ag SAC solders such as SAC125 and SAC105 at lower strain rates when compared to drop test results in literature.

REFERENCES

1. Ganesan, S. and Pecht, M. G., "Lead-free electronics". Wiley-IEEE Press, 2006.
2. Kim, H., Zhang, M., Kumar, C.M., Suh, D., Liu, P., Kim, D., Xie, M., Wang, Z., "Improved drop reliability performance with lead free solders of low Ag content and their failure modes", Electronic Components and Technology Conference, vol. 57, pp 962-967, 2007.
3. Dudek, R., Faust, W., Wiese, S., Rollig, M., Michel, B., "Low-cycle fatigue of Ag-based solders dependent on alloying composition and thermal cycle conditions", Electronics Packaging Technology Conference, vol. 9, pp 14-20, 2007.
4. Chong, D.Y.R., Ng, K., Tan, J.Y.N., Low, P.T.H., Pang, J.H.L., Che, F.X., Xiong, B.S., Xu, L.H., "Drop impact reliability testing for lead-free and leaded soldered IC packages", Electronic Components and Technology Conference., vol. 55, pp 622-629, 2005.
5. Zhu, W.H., Xu, L., Pang, J.H.L., Zhang, X.R., Poh, E., Sun, Y.F., Sun, A.Y.S., Wang, C.K., Tan, H.B., "Drop reliability study of PBGA assemblies with SAC305, SAC105 and SAC105-Ni solder ball on Cu-OSP and ENIG surface finish", Electronic Components and Technology Conference, vol. 58, pp 1667-1672, 2008.
6. Liu, W, Bachorik, P., Lee, N.C., "The superior drop test performance of SAC-Ti solders and its mechanism", Electronic Components and Technology Conference, vol. 58, pp 452-458, 2008.
7. Wong, E.H., Seah, S.K.W., Selvanayagam, C.S., Rajoo, R., van Driel, W.D., Caers, J.F.J.M., Zhao, X.J., Owens, N., Leoni, M., Tan, L.C., Lai, Y.-S., and Yeh, C.L., "High-speed cyclic bend tests and board-level drop tests for evaluating the robustness of solder joints in printed circuit board assemblies", Journal of Electronic Materials, vol 38, no. 6, pp 884-895, 2009.
8. Zhan, C.J., Chuang, C.C., Chang, T.C., Shen L.C., "The performance of various solder ball under high shear speed test", International Microsystems Packaging Assembly and Circuits Technology, pp 66-70, 2007.
9. Song, F., Lee, S.W.R., Newman, K., Reynolds, H., Clark, S., Sykes, B., "Effect of thermal aging on high speed ball shear and pull tests of SnAgCu lead-free solder balls", Electronics Packaging Technology Conference, vol. 9th., pp 463-470, 2007.
10. Suh, D., Kim, D.W., Liu, P., Kim, H., Weninger, J. A., Kumar, C.M., Prasad, A., Grimsley, B.W., Tejada, H.B., "Effects of Ag content on fracture resistance of Sn-Ag-Cu lead-free solders under high-strain rate conditions", Materials Science and Engineering, vol. 460-461, pp 595-603, 2007.
11. Reid, M., Punch, J., Collins, M., Ryan, C., "Effect of Ag content on the microstructure of Sn–Ag–Cu based solder alloys", Conference on Soldering and Surface Mount Technology, pp 3–8, 2008.
12. Liu, Y., Kessels, F.J.H.G., van Driel, W.D., van Driel, J.A.S., Sun, F.L., Zhang, G.Q., "Comparing drop impact test method using strain gauge measurements", Microelectronics Reliability, vol. 49, no. 9-11, pp 1299-1303, 2009.
13. Khatibi, G., Wroczewski, W., Weiss, B., Ipser, H., "A novel accelerated test technique for assessment of mechanical reliability of solder interconnects", Microelectronics Reliability, vol. 49, no. 9-11, pp 1283-1287, 2009.
14. Osterman, M.; Dasgupta, A.; Han, B., "A strain range based model for life assessment of Pb-free SAC solder interconnects", Electronic Components and Technology Conference, vol. 56, pp 7, 2006.
15. Suhling, J.C., Gale, H.S., Johnson, R.W., Islam, M.N., Shete, T., Lall, P., Bozack, M.J., Evans, J.L., Seto, P., Gupta, T., Thompson, J.R., "Thermal cycling reliability of lead free solders for automotive applications", The

Ninth Intersociety Conference on Thermal and Thermo-mechanical Phenomena in Electronic Systems, vol. 2, pp 350- 357, 2004.
16. Fan, X., Raiser, G., Vasudevan, V.S., "Effects of dwell time and ramp rate on lead-free solder joints in FCBGA packages", Electronic Components and Technology Conference, vol. 55, pp 901-906, 2005.
17. Zhong, Z.W., "Thermal strain analysis of IC packages using various Moiré methods", Microelectronics International, vol. 21, no. 3, pp. 25-28, 2004.
18. "Guidelines for accelerated reliability testing of surface mount solder attachments", IPC-SM-785 Association Connecting Electronics Industries, 1992.
19. Zubelewicz, A., Tokarz, R., Kuracina, R, and McGinniss, J., "Mechanical Deflection System- An Innovative Test Method for SMT Assemblies", Advances in Electronic Packaging, ASME, vol. 10, no. 2, pp. 1167-1177, 1995.
20. Filho, W.C.M., Brizoux, M., Fremont, H., Danto, Y., "Solder Joint Loading Conditions under Torsion Test," Seventh International Conference on Thermal, Mechanical and Multiphysics Simulation and Experiments in Micro-Electronics and Micro-Systems, pp. 1-6, 2006.
21. Pang, J.H.L., Ang, K.H., Shi, X.Q., Wang, Z.P., "Mechanical deflection system (MDS) test and methodology for PBGA solder joint reliability," IEEE Transactions on Advanced Packaging, vol. 24, no. 4, pp. 507-514, 2001.
22. Srinivas, V., Al-Bassyiouni, M., Osterman, M., Pecht, M., "Characterization of lead-free solder interconnects reliability under torsional loads", International Mechanical Engineering Congress & Exposition, ASME, 2009.
23. Srinivas, V., Osterman, M., Farell, R., Pecht, M., "Reliability evaluation of one-pass and two-pass techniques of assembly for package on packages under torsion loads", APEX EXPO, IPC, 2010.
24. Qi, H., Zhang, Q., Tinsley, E.C., Osterman, M., Pecht, M., "High cycle cyclic torsion fatigue of PBGA Pb-free solder joints", IEEE Transactions on Components and Packaging Technologies, vol. 31, no. 2, pp 309-314, 2008.
25. Gu, J., Barker, D., Pecht, M., "Prognostics implementation of electronics under vibration loading", Microelectronics Reliability, vol. 47, no. 12, Electronic System Prognostics and Health Management, pp 1849-1856, 2007.
26. "Guidelines for performance test methods and qualification requirements for surface mount solder attachments", IPC-9701, 2002.